Capacity of MIMO Systems Based on Measured Wireless Channels

Andreas F. Molisch, *Senior Member, IEEE*, Martin Steinbauer, *Associate Member, IEEE*,
Martin Toeltsch, *Student Member, IEEE*, Ernst Bonek, *Senior Member, IEEE*, and
Reiner S. Thomä, *Senior Member, IEEE*

Abstract—We measure the capacity of multiple-input multiple-output radio systems in microcellular environments. We use a new data evaluation method that allows to evaluate the cumulative distribution function of the capacity from a single measurement. This method is based on an extraction of the parameters of the multipath components and, thereafter, a synthetic variation of their phases. In the analyzed environments, we find capacities to be about 30% smaller than would be anticipated from an idealized model. In addition, the frequency selectivity of the channel makes the cdf of the capacity steeper and, thus, increases the outage capacity, compared with the frequency-flat case, but the influence on the mean capacity is small.

Index Terms—Multipath channels, multiple-input multiple-output, radio propagation.

I. INTRODUCTION

MIMO (multiple-input multiple-output) wireless systems have multiple antennas at both transmitter and receiver. In contrast to conventional smart antennas, which improve the quality of a single data stream, a MIMO system provides multiple independent transmission channels, thus, leading (under certain conditions) to a channel capacity that increases linearly with the number of antenna elements. This fact was first recognized by simulations in the late 1980s [1], but gained large attention mainly with the publication of analytical results in the mid-1990s [2]–[4]. Since that time, the interest in MIMO systems has exploded. Space-time codes that come reasonably close to realizing this capacity have been proposed [5], [6], and commercial products based on such ideas are currently under development [7]

Right from the beginning, it was realized that the nature of the channels, its statistical properties, and the correlation of the antenna elements will decide whether the predicted capacities can

be reached in reality. So MIMO measurements are desperately needed, although they are quite cumbersome and difficult to make. Previous theoretical work is based on simplified channel models. Most references assumed that the signal at each antenna element is Rayleigh fading and uncorrelated with the fading at all antenna elements. Such a channel, which requires a rich multipath environment, is good for MIMO systems, because it guarantees the existence of independent transmission channels.[1] Reference [8] discussed various physical conditions for the decorrelation condition to hold, and how the capacity changes if these are not fulfilled. [9] and [10] investigated the effect of deviations from the standard model. They assumed local scattering around the mobile station (MS), with a rather small angular spread as seen from the base station (BS) [11], [12]—an assumption that is often fulfilled for macrocells, but not for micro- and picocells. All the above mentioned investigations are for the flat-fading case, while [13] also investigated the effect of time dispersion with the macrocell model of [12]. Recent investigations [14], [15] also indicate that there are certain channel configurations (termed "keyholes" of "pinholes") where the capacity is dramatically lower than in the independent-Rayleigh-fading case.

The earlier theoretical work assumed frequency-flat fading channels. Recently, interest has turned to the performance in frequency-selective channels, e.g., [13], [16]. There are two reasons for this interest: 1) MIMO systems are especially suitable for high-data-rate communications, which inherently cover larger bandwidths and, thus, usually encounter frequency-selective channels; and 2) the frequency diversity inherent in frequency-selective channels can be exploited to additionally increase the outage capacity of the system. Again, this additional improvement depends on the details of the channel model.

In contrast to all those theoretical efforts, little is known about capacity evaluations based on measurement campaigns. One reason for this is certainly the expense and inconvenience of performing double-directional measurement campaigns, which are one step up from the already difficult directional measurements at BS or MS [17]. To alleviate this problem, we propose in this paper a new procedure that allows to evaluate the cumulative distribution function (cdf) of the capacity from a single MIMO channel snapshot. We apply the procedure to the evaluation of a measurement campaign in microcells.

Thus, the major contributions of this paper are the following.

 1) We present a new method to extract, from a single measurement, a MIMO radio channel parametrization that al-

[1]For many years, it had been believed that mobile radio channels with a high degree of multipath scattering are hostile and inherently "bad" channels.

lows the determination of the cdf of the capacity. It is based on the determination of the directions-of-arrival (DOAs), direction-of-departure (DODs), and delays of the multipath components, coupled with a synthetic variation of their phases. This procedure allows a drastic reduction of the measurement effort.

2) We apply this method to measurements at 5.2 GHz both for the frequency-flat and the frequency-selective channel. From this, we derive:

   a) results for the capacity of *frequency-flat* channels in microcellular environments, and investigate the effects of the number of antennas, and other parameters;

   b) we derive similar results for *frequency-selective* channels, and show how the mean capacity and outage capacity are improved as the bandwidth is increased.

From this, we can draw conclusions about how to model the MIMO channel best to capture its essential properties.

The rest of the paper is organized the following way. In Section II, we present the measurement setup and the environments covered by our measurement campaigns. The algorithms that we used for the extraction of the parameters of the multipath components are described in Section III. Next, we describe the principle of our capacity evaluation approach, both for the frequency-flat and the frequency-selective channel, and discuss its general applicability. Section V gives the results of our evaluation, and discusses the influence of the various parameters on our results. A summary concludes the paper.

II. MEASUREMENT SETUP

We performed a measurement campaign in two courtyards in Ilmenau, Germany. We measured in the 5.2-GHz band, as this has been assigned for wireless local area networks (LANs), e.g., HIPERLAN (see www.etsi.org), or IEEE 802.11a. These standards specify wireless communication between computers, which is a compelling application for MIMO systems. Our measurement device was a RUSK ATM channel sounder with a bandwidth of 120 MHz, connected via a fast RF switch to a uniform linear receiver antenna array. This array consisted of $N_R = 8$ antenna elements ($\pm60°$ element-beamwidth), plus two dummy elements at each end of the array. All these components together constitute a single-directional channel sounder that is described in more detail in [18]. To perform double-directional measurements, we also need an array of transmit antennas. For simplicity as well as versatility, we decided on a virtual array at the transmitter. It consists of a monopole antenna mounted on a X–Y-positioning device with stepping motors. The positioning was controlled by a personal computer (PC) via a serial RS 232 interface.

The raw data were acquired using a two-sided multiplexing technique [19]. We positioned the transmit antenna at a certain position, and started to sound the channel. At the receiver, the RF switch was connected to the first antenna element of the array, so that we sounded the transfer function (measured at
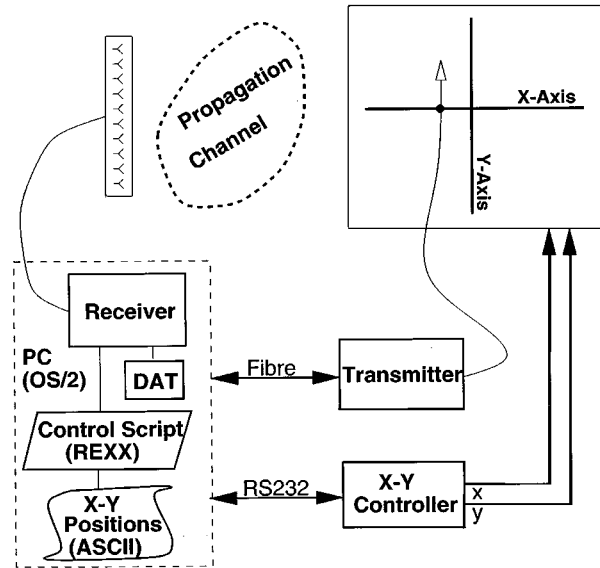

Fig. 1. Measurement setup with double array multiplexing for sounding the double-directional radio channel.

192 frequency samples) from the first transmit to the first receive element of our array. Then, the switch was connected to the next receive antenna element, and the next transfer function was measured. The measurement of all those transfer functions was repeated 256 times, in order to assess the time variance of the channel (see below). Then, the transmit antenna was moved to the next position, and the procedure was repeated. For the multipath parameter evaluation, we used $N_T = 16$ transmit antenna positions that were situated on a cross (i.e., 8 positions on each axis of the cross) and recorded bursts of complex channel transfer functions. The regularly sampled data (in frequency, time and two spatial domains) were buffered on a harddisk, stored on a digital audio tape (DAT)-tape, and later transferred to the PC.

For a correct extraction of the multipath parameters, transmitter and receiver must be properly synchronized in time and frequency. This was achieved by connecting transmitter (TX) and receiver (RX) by an optical fiber. The effect of signal runtime through the fiber and the signal processing delays were eliminated by back-to-back calibration. The measurement setup is shown in Fig. 1.

Any virtual array requires that the channel remains static during the measurement period. In our case, one complete measurement run (2×8 antenna positions at TX times 8 spatial samples at RX times 192 frequency samples and 256 temporal samples gives $16 \times 8 \times 192 \times 256 = 6.291.456$ complex samples) took about 5 minutes. To assure the time-invariance during that period, we used two procedures: the first one was a Doppler-filtering procedure (see Section III). Secondly, we performed measurements in the same location three times at intervals of about 5–10 min, and compared the results.

On the other hand, there are two compelling advantages of the virtual array-technique: 1) it is more versatile than the physical-array arrangement; and 2) there is no mutual coupling to neighboring elements, so that no calibration is required.

III. DATA EVALUATION

We will see that for our new evaluation of the capacity, we need not the transfer function from each element to each next one, but rather the parameters [(delays, directions of arrival (DOAs), directions of departures (DODs)] of the multipath components. There is a wealth of methods available for this task. For the extraction of delays, the usual Fourier transform with Hanning windowing would yield sufficiently accurate estimates, since our measurements were performed with a very high bandwidth. However, DOA estimation from spatially sampled data by Fourier methods would yield low accuracy in the DOA and DOD estimation, since the number of antenna elements is rather low. Due to this reason, superresolution algorithms are required [20]. These algorithms assume a parametric model for the incident signal (to wit, a sum of planar waves), and use the measured signal to extract its parameters. The limitations of superresolution algorithms do not lie in the resolution, but rather in the number of waves multipath components (MPCs) that they can estimate. We will see that it is beneficial to apply a superresolution algorithm not only for the DOAs and DODs, but also the delay estimation. In principle, a sequential or joint estimation [21], [22] of the parameters is possible—we used the sequential approach in our evaluations.

Starting from the four-dimensional transfer function (time, frequency, position of RX antenna, position of TX antenna), we first compute the Doppler-variant transfer function by Fourier transforming the 256 temporal samples (with Hanning windowing). Next, we eliminate all components that do not exhibit zero Doppler shift (Doppler filtering). Those components correspond, e.g., to MPCs scattered by leaves moving in the wind, as we made sure that no moving persons or machinery were in the measured courtyard. The eliminated components carry on the order of 1% of the total energy. The three-dimensional (static) transfer function obtained in that way is then evaluated by unitary estimation of signal parameters by rotational invariance techniques (ESPRIT) [23] to estimate the delays τ_i. Unitary ESPRIT is an improved version of the classical ESPRIT algorithm [24]. They both estimate the signal subspace for extraction of the parameters of (spatial or frequency) harmonics in additive noise. One important step in ESPRIT is the estimation of the model order. Different methods have been proposed in the literature for that task. We used the relative power decrease between neighboring eigenvalues with additional correction by visual inspection of the *Scree Graph* showing the eigenvalues.

After estimation of the parameters τ_i, we can determine the corresponding "steering" matrix A_τ. Subsequent beamforming with its Moore–Penrose pseudoinverse [25] A_τ^+ gives the vector of delay-weights for all $\vec{x}_R, \vec{x}_T$

$$\vec{h}_\tau(\vec{x}_T, \vec{x}_R) = \mathbf{A}_\tau^+ \, \vec{T}_f(\vec{x}_T, \vec{x}_R) \tag{1}$$

where $\vec{T}_f$ is the vector of transfer coefficients at the 192 frequency subbands sounded. This gives us now the transfer coefficients from all positions $\vec{x}_T$ to all positions $\vec{x}_R$ separately for each delay τ_i. Thus, one dimension, namely the frequency, has been replaced by the *parameterized* version of its dual, the delays.
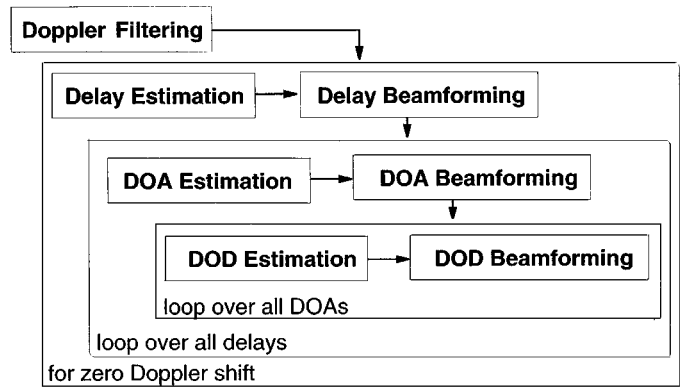

Fig. 2. Sequential estimation of the parametric channel response in the different domains: alternating estimation and beamforming.

For the estimation of the DOA in each of the two-dimensional transfer functions, we apply ESPRIT estimation and beamforming by the pseudoinverse

$$\vec{h}_{\varphi_R}(\tau_i, \vec{x}_T) = \mathbf{A}_{\varphi_R}^+ \, \vec{h}_{x_R}(\tau_i, \vec{x}_T). \tag{2}$$

Finally for the DOD

$$\vec{h}_{\varphi_T}(\tau_i, \varphi_{R,i,j}) = \mathbf{A}_{\varphi_T}^+ \, \vec{h}_{x_T}(\tau_i, \varphi_{R,i,j}). \tag{3}$$

The whole evaluation procedure is sketched in Fig. 2. It gives us the number and parameters of the MPCs, i.e., the number and values of delays, which DOA can be observed at these delays and which DOD corresponds to each DOA at a specific delay. Furthermore, we also obtain the powers of the MPCs. One important point in the application of the sequential estimation procedure is the sequence in which the evaluation is performed. Roughly speaking, the number of MPCs that can be estimated is the number of samples we have at our disposal. It is thus vital to first evaluate the frequency domain, since we had two samples available.[2] Estimating DOAs in a first step would strongly limit the number of resolvable MPCs. As we will see below, the number of strong MPCs, as determined from the scree graph, was on the order of 30. This could be resolved with the available frequency samples.

More details about the evaluation procedure can be found in [26].

IV. CAPACITY COMPUTATION

A. The Key Idea

In a fading channel, the capacity is a random variable, depending on the local (or instantaneous) channel realization. In order to determine the cdf of this capacity and, thus, the outage capacity, we would have to perform a large number of measurements either with slightly displaced arrays, or with temporally varying scatterer arrangement. Since each single measurement requires a huge effort, such a procedure is highly undesirable.

---

[2]Actually, we had to perform a smoothing over subarrays (equivalent to spatial smoothing) first. In the frequency domain, the size of the subarrays was 64, so that 129 samples remained—still more than enough to resolve all dominant MPCs. In the spatial domains, the size of the subarrays was four.

To improve this situation, we propose a new evaluation technique that requires only a *single* measurement of the channel. This technique relies on the fact that we can generate different realizations of the transfer function by changing the *phases* of the multipath components. It is a well-established fact in mobile radio that these phases are uniformly distributed random variables, whose different realizations occur as either transmitter, receiver, or scatterers move [27]. We can, thus, generate different realizations of the transfer function from the mth transmit to the kth receive antenna as

$$h_{k,m}(f) = \sum_i a_i \exp\left(-j\frac{2\pi}{\lambda}d\left[k\sin(\phi_{R,i}) + m\sin(\phi_{T,i})\right]\right)$$
$$\times \exp(-j2\pi f \tau_i)\exp(j\alpha_i) \quad (4)$$

where α_i is a uniformly distributed random phase, which can take on different values for the different MPCs numbered i. Note, however, that α_i stays unchanged as we consider different antenna elements k and m. To simplify discussion, we for now consider only the flat-fading case, i.e., $\tau_i = 0$.

We can, thus, generate different realizations of the channel matrix $\mathbf{H}$

$$\mathbf{H} = \begin{pmatrix} h_{11} & h_{12} & \dots & h_{1N_T} \\ h_{21} & h_{22} & \dots & h_{2N_T} \\ \dots & \dots & \dots & \dots \\ h_{N_R 1} & h_{N_R 2} & \dots & h_{N_R N_T} \end{pmatrix} \quad (5)$$

by the following two steps.

1) From a single measurement, i.e., a single snapshot of the channel matrix, determine the DOAs, and DODs of the MPCs as described in Section III;
2) Compute synthetically the impulse responses at the positions of the antenna elements, and at different frequencies. Create different realizations of one ensemble by adding random phase factors (uniformly distributed between 0 and 2π) to each MPC.

For each channel realization, we can compute the capacity[3] from [3]

$$C = \log_2 \det\left(\mathbf{I} + \frac{\rho}{N_T}\mathbf{H}^H\mathbf{H}\right) \quad (6)$$

where ρ denotes the signal-to-noise ratio (SNR). $\mathbf{I}$ is the identity matrix and superscript H means Hermitian transposition.

B. Frequency-Selective Case

For the frequency-selective case, we have to evaluate the capacity by integrating over all frequencies. In the following, we consider the channel capacity per unit bandwidth (dimension bit/s/Hz):

$$C = \frac{1}{B}\int_B \log_2 \det\left(\mathbf{I} + \frac{\rho}{N_T}\mathbf{H}^H(f)\mathbf{H}(f)\right)df. \quad (7)$$

Here, $\mathbf{H}(f)$ is the frequency-dependent transfer matrix. The integration range is the bandwidth of interest.

---

[3]This is the capacity when the channel is unknown to the transmitter, so we assume the transmit power to be equally distributed over all TX antennas, as no waterfilling can be employed. Our procedure for generating capacity cdfs is, however, also valid for the case of known channels, where an appropriately modified capacity equation [28] is to be used.
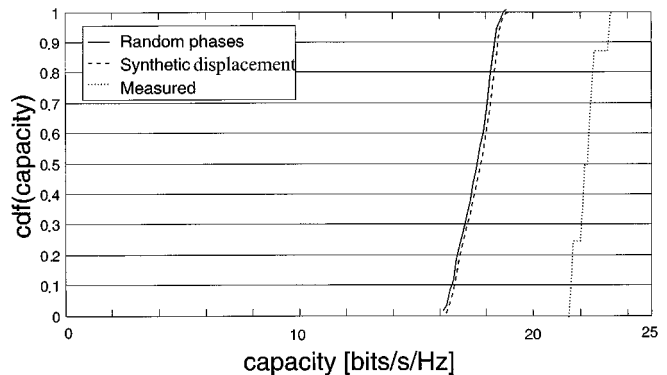

Fig. 3. Cdf of capacity in Scenario II with eight antenna elements and 20 dB SNR. Uniformly distributed random phases (solid), synthetic transmitter displacement (dashed), and measured transmitter displacement (dotted).

C. Validation

Despite the intuitive appeal of ascribing uniformly distributed random phases to the MPCs, further experimental validation is desirable. For this, we proceed in two steps.

1) We establish that, in our case, ascribing uniformly distributed phases gives the same capacity cdf as moving the transmitter synthetically over a given range.
2) We establish to what extent the cdf with the synthetic transmitter movement can be reproduced experimentally.

A movement of the transmitter position can be easily emulated in the computation of our transfer function. The only condition is that the DODs and delays do not change significantly as we move the transmitter.[4] By transposing (displacing) and/or rotating the antenna arrays, we can, thus, create different realizations of the channel. The resulting cdf can then be compared with the cdf as computed by the method of Section IV-A. Fig. 3 shows one example of such a comparison (solid and dashed lines) in Scenario II. We see excellent agreement.

The second step is the comparison of the synthetic receiver movement to actual measurement results of the capacity. We measured the transfer function with eight different linear synthetic transmit arrays, displaced (in the direction orthogonal to the orientation of the array) by multiples of half the wavelength. As we have only eight samples of the channel *matrix*, the cdfs exhibit a strong "staircase" characteristic (dotted line in Fig. 3). It is noticeable that the capacity as obtained from the direct measurements is larger than the synthetically obtained capacity.

There are several effects that can lead to a difference between directly measured capacities and capacities based on extracted MPC parameters. We investigated the following possibilities:

- The *basic correctness* of the evaluation programs. This was checked by analyzing known synthetic data.
- The *influence of the beamforming algorithm* (see Section III) on the obtained powers of the MPCs. We analyzed this by applying different beamformers (apart from the simple Moore–Penrose pseudoinverse), but did not observe a significant effect on the capacity. Note, however, that the identification of the MPC powers is best done in the first step of the sequential ESPRIT algorithm,

---

[4]Actually, the delays do not play a role for the flat-fading case, but become relevant for the frequency-selective case described below.
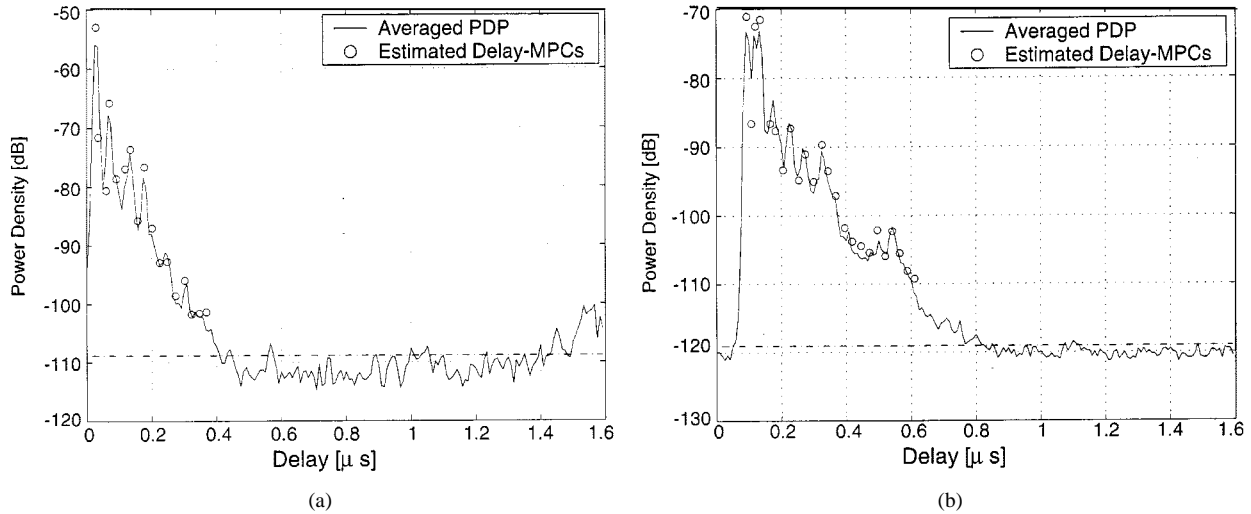
Fig. 4. Power delay profiles (lines) (a) in the LOS Scenario I and (b) in the obstructed LOS Scenario IV. Superimposed (circles) are the identified MPCs that are further used to compute the simulated capacities.

as beamforming errors tend to accumulate, and can lead to serious mis-estimation of the signal powers[5].

- The influence of the estimated *number of multipath components.* As mentioned in Section III, the estimation of the channel rank is one of the most important, but also most difficult problems of high-resolution algorithms. We tested different ranks of the channel—however, the influence on the measured capacities was minor.

- The influence of *noise.* Noise in the directly measured data enhances the capacity, as it leads to uncorrelated contributions to the scattering function. For the line-of-sight (LOS) scenarios (Scenario I and II), an effective SNR on the order of 20 dB would be required to explain the discrepancy between directly measured capacities and random-phase-generated capacities. For Scenarios III and IV, effective SNRs of 7 dB and 10 dB, respectively, would be required. However, we note that the SNR of our measurement system was much better.[6]

- The impact of the *powers* of the obtained multipath components. We compared them to the powers obtained from the directly measured data (transfer functions). By Parseval's theorem, they should converge to the same values as the number of samples tends to infinity. However, we found that the total powers of the MPCs were noticeably lower. The ratio of the "unaccounted" power (i.e., power not ascribed to a MPC) over the total power was −20 dB in Scenarios I and II, but −6 and −10 dB in Scenarios III and IV.

From the above, we conclude that, due to both noise and unaccounted MPCs, the effective SNR is rather low, and we were not able to identify which part of the parameter extraction algorithm was responsible for "losing" some of the power. If, however, we added the unaccounted power as "equivalent" noise in our parametric model, we would get very good agreement between directly-measured capacities and parameter-based capacities.

---

[5]Note that the capacity plots given in [29] are based on such accumulated power estimates.

[6]Independently from our investigations, [30] has treated the influence of noise on the capacity.

Our "random phase" method works, in principle, for an arbitrary number of antennas. As long as the MPCs can be determined (e.g., in the delay domain), even the capacities of arrays *larger* than the measurement array can be analyzed. We stress, however, that the effects of unresolved MPCs on the capacity become stronger as the number of antennas increases (see also Section V, Fig. 8).

V. RESULTS

A. Measurement Environments

The following scenarios were evaluated with the procedure described above:

- *Scenario I: A courtyard with dimensions 26 m × 27 m, open on one side.* The RX-array broadside points into the center of the yard, the transmitter is located on the positioning device 8 m away in LOS. The power delay profile (PDP) in this scenario is given in Fig. 4 (left plot).

- *Scenario II: Closed backyard of size 34 m × 40 m with inclined rectangular extension.* The RX-array is situated in one rectangular corner with the array broadside of the linear array pointing under 45° inclination directly to the middle of the yard. The LOS connection between TX and RX measures 28 m. Many metallic objects are distributed irregularly along the building walls (power transformers, airconditioned fans, etc.). This environment looks very much like the backyard of a factory (Fig. 5).

- *Scenario III: Same closed backyard as in II but with artificially obstructed LOS path.* It is expected that the metallic objects generate serious multipath and higher order scattering that can only be observed within the dynamic range of the device if the LOS path is obstructed.

- *Scenario IV:* Same as Scenario III but with different TX position and LOS obstructed. The TX is situated nearer to the walls. Fig. 4 (right plot) gives the measured power delay profile. The PDPs in Scenarios II and III look similar, besides the LOS component that occurs dominantly for Scenario II. More details about the scenarios can be found in [26].
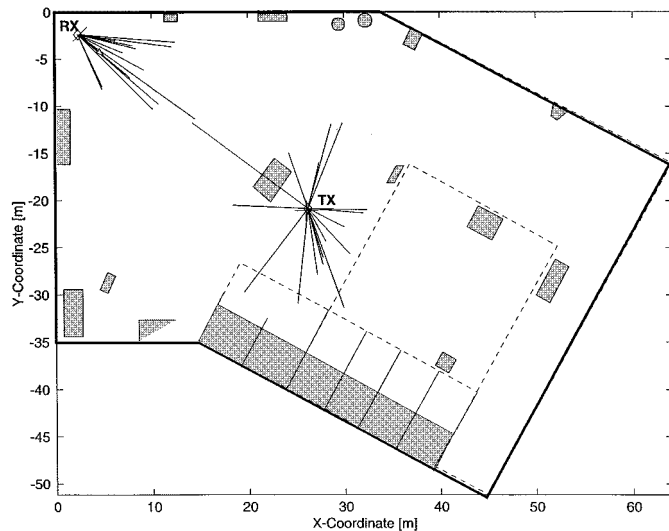
Fig. 5. Geometry of the environment of Scenario II to IV (backyard) in top view. Superimposed are the extracted DOAs and DODs for Scenario III.
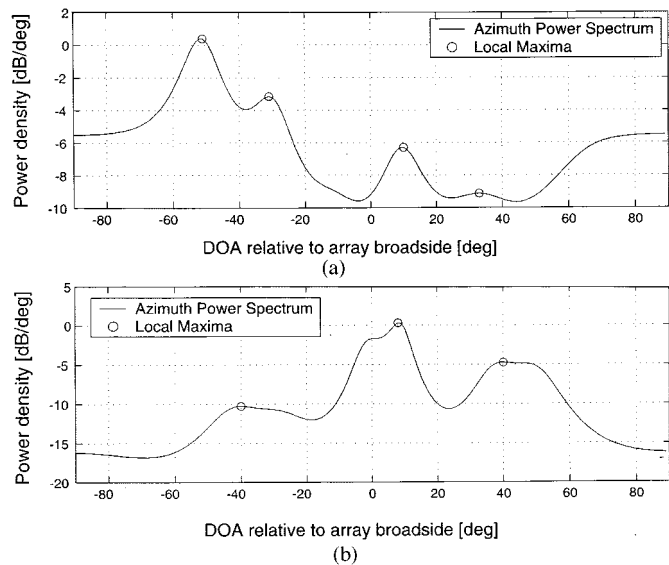

Fig. 6. Azimuthal power spectra at (a) the transmitter and (b) receiver for Scenario III (obstructed LOS). Spectra computed with minimum variance method (MVM, Capon's beamformer). Angles refer to array broadside, so that (due to array position) $+8°$ and $-53°$ correspond.

Fig. 6 shows the azimuthal power spectra at (a) the transmitter and (b) the receiver for Scenario III (obstructed LOS). Shown is the nonambiguous angle range of $180°$ w.r.t. broadside for the linear arrays used in the capacity computation. As can be seen, the power is distributed approximately uniformly at the transmitter, where we took the spatial samples of the capacity. Even though the distance between the sampling points was only half a wavelength, this angular spectrum assures that even neighboring samples (i.e., samples spaced half a wavelength apart) are approximately decorrelated. It can also be seen that the obstruction of LOS was not sufficient to remove this component entirely. This is reflected by the maximum of the spectra, which corresponds well to the LOS direction.
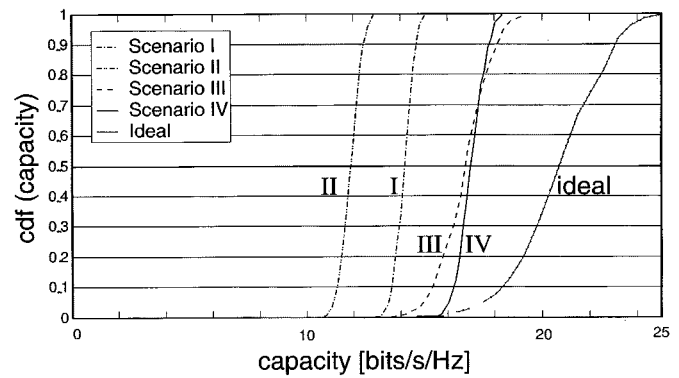

Fig. 7. Cdfs of the MIMO channel capacity encountered in Scenarios I–IV, and the cdf for an ideal channel. The SNR is 20 dB and 4×4 antenna elements were used.

B. Capacity Distribution in Flat-Fading Channels

First, we consider the capacity cdf of the flat-fading channels as evaluated by the method of Section IV-A. We assume linear antenna arrays with 4 elements each at transmitter and receiver, and an SNR of 20 dB. In our environments, we find a 10% outage capacity on the order of 11–16 bits/s/Hz (see Fig. 7) compared with more than 18 bit/s/Hz in the ideal channel.[7] Furthermore, we also observe that the capacity varies considerably from one environment to the next. In those cases where a LOS exists, the capacity is lower than for the NLOS situations (however, the comparison made above is not really fair: in a LOS environment, the SNR will usually be much higher than in a NLOS environment). Finally, we observe that all measured cdfs are steeper than the "ideal" cdf—especially in Scenarios I and II. This is related to the existence of a few dominant components. In Scenarios I and II, a single component (the LOS component) carries most of the power, while in Scenarios III and IV, a few components with small delay carry most of the power. The "ideal" cdf can only be obtained by a large number of components with approximately equal power. We also observe that the properties of our measured channel lead to a loss (compared with the ideal channel) of *outage capacity* that is smaller than the loss of *mean capacity*.

Further simulations showed that the measured outage capacity exhibited no significant increase if we increased the inter-element spacing above $\lambda/2$. A similar observation was made in [31] for the case of spatially uniformly distributed scatterers between transmitter and receiver. This indicates that decorrelation via the phases is not the limiting factor for our capacities. Rather, the relatively small number of MPCs, and especially the different powers carried by them, limits C. We checked this conjecture by using the measured DOAs and DODs, but assigning equal power to the MPCs, and got capacities very similar to the "ideal" case.

Fig. 8 reports the effect on the capacity when increasing the number of antenna elements at both link ends ($N_T = N_R$). It can be seen clearly that the capacity gain per additional antenna element is much larger for the NLOS than for the LOS case, a result that is in line with the reasoning of [8]. We also observe

---

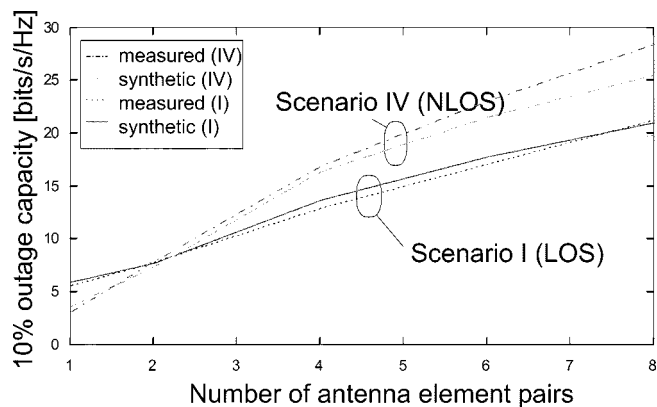[7]The "ideal" MIMO channel results from independent identically distributed complex Gaussian entries in the transfer matrix.

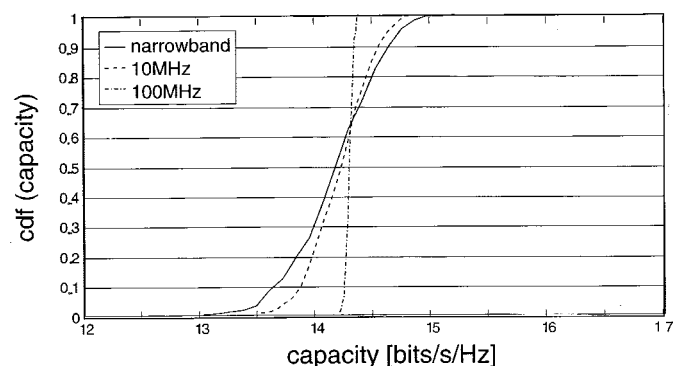Fig. 8. Outage capacity at 10% level in Scenarios I (LOS) and IV (LOS) over the number of antenna element pairs.

Fig. 9. Capacity of a 4×4 antenna arrangement in Scenario I at different bandwidths and $\mathrm{SNR} = 20$ dB.

that for a small number of antenna elements, the outage capacity of the LOS case is larger than for the NLOS case, while this is reversed for a large number of antenna elements. We also see that the effect of noise or unaccounted-for power on the capacity becomes larger with a larger number of antenna elements, as expected.

C. Frequency-Selective Channels

Fig. 9 shows the gain in mean capacity and outage capacity in Scenario I as we increase the bandwidth. Essentially, we would expect a gain in the outage capacity as we increase the bandwidth (note that we normalize the capacity to unit bandwidth in all cases). This should occur because the frequency selectivity of the channel adds additional diversity, so that the *outage* capacity becomes closer to the *mean* capacity. In Scenario I, the outage capacity improves from 13.6 bits/s/Hz to 14.2 bits/s/Hz indeed, when we increase the bandwidth from narrowband to 100 MHz, and to 13.8 bits/s/Hz when the bandwidth is a (more realistic) 10 MHz. As could be anticipated, the correlation bandwidth of the channel thus has an important influence on the improvement of the outage capacity.

Another interesting point is the improvement of the mean capacity by using wideband transmission in a frequency-selective channel. For the single-antenna case, it is well-known that the mean capacity is not improved by frequency diversity. However, [10] has shown theoretically that, in MIMO systems, the frequency selectivity of the channel can increase also the
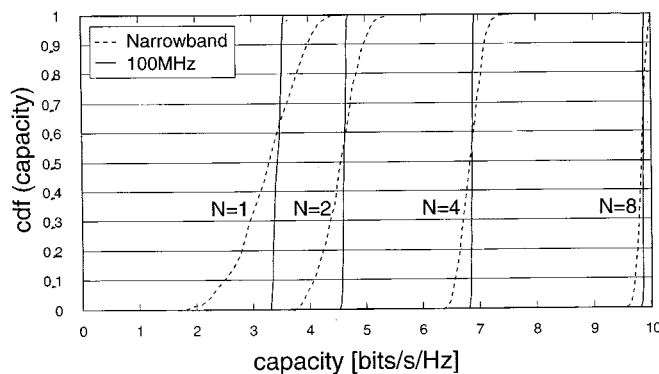

Fig. 10. Capacity distribution for narrowband case (dashed) and 100 MHz bandwidth (solid) and 10 dB SNR in Scenario I for array sizes $N_T = N_R = 1, 2, 4, 8$.

mean capacity. Increases up to 30% were predicted for certain channel situations. However, in our measurements, we found only a small change in the mean capacity as we increased the bandwidth and, thus, the frequency selectivity. Specifically, the increase was always less than 10%. This is probably due to the fact that the scatterer distribution in our scenarios differed appreciably from the one assumed in [10].

Finally, we investigate the improvement of the outage capacity by frequency diversity as a function of the array size. We find that both the relative and the absolute improvement decreases as the number of antennas increases, see Fig. 10. The reason for this behavior is that the additional antennas already provide some degree of diversity, so that the additional frequency diversity becomes less important.

VI. SUMMARY AND CONCLUSION

We have presented measurements of the channel capacity of MIMO systems, and shown how a parametric channel model allows the evaluation of the complete cdf, and the outage capacities at arbitrary outage levels. Our new method is based on first extracting the parameters of the MPCs from one measurement snapshot, and then obtaining different channel realizations by assigning random phases to the MPCs. This method has been both physically justified and tested against measurement results. The parametric channel representation, together with the random-phase technique, is much more versatile than conventional representations. For example, we can analyze the influence of the channel on MIMO systems with more antennas than the channel sounding equipment, or with different antenna configurations.

We then showed important properties of measured channels in two courtyards. We identified the channel properties that most strongly influence the capacity in those environments. We found that despite an almost uniform distribution of the DOAs and DODs, the capacities are up to 30% lower than would be expected from a simple model. We also showed that in the considered environments, a transmission bandwidth of 100 MHz is required to make the cdf *de facto* a step function, with 10 MHz giving only half the improvement in outage capacity. Finally, we found no significant increase in the mean capacity even for very large bandwidths.

Naturally, numerous measurement campaigns in many different environments will be needed in the future before a complete understanding of the double-directional channel and the resulting capacities is achieved.

REFERENCES

[1] J. H. Winters, "On the capacity of radio communications systems with diversity in Rayleigh fading environments," *IEEE J. Select. Areas Commun.*, vol. 5, pp. 871–878, June 1987.

[2] G. J. Foschini, "Layered space-time architecture for wireless communication in a fading environment when using multi-element antennas," *Bell Labs Techn. J.*, pp. 41–59, Autumn 1996.

[3] G. J. Foschini and M. J. Gans, "On limits of wireless communications in fading environments when using multiple antennas," *Wireless Personal Commun.*, vol. 6, pp. 311–335, 1998.

[4] J. B. Andersen, "Antenna arrays in mobile communications: Gain, diversity, and channel capacity," *IEEE Antennas Propagat. Mag.*, pp. 12–16, Apr. 2000.

[5] V. Tarokh, N. Seshadri, and A. R. Calderbank, "Space-time codes for high data rate wireless communication: Performance criterion and code construction," *IEEE Trans. Inform. Theory*, vol. 44, pp. 744–765, 1998.

[6] V. Tarokh, A. Naguib, N. Seshadri, and A. R. Calderbank, "Space-time codes for high data rate wireless communication: Performance criteria in the presence of channel estimation errors, mobility, and multiple paths," *IEEE Trans. Commun.*, vol. 47, pp. 199–207, 1998.

[7] H. Boelcskei, A. J. Paulraj, K. V. S. Hari, R. U. Nabar, and W. W. Lu, "Fixed broadband wireless access: State of the art, challenges, and future directions," *IEEE Commun. Mag.*, pp. 100–108, 2001.

[8] P. F. Driessen and G. J. Foschini, "On the capacity formula for multiple input–multiple output wireless channels: A geometric interpretation," *IEEE Trans. Commun.*, vol. 47, pp. 173–176, 1999.

[9] D. Shiu, G. Foschini, M. Gans, and J. Kahn, "Fading correlation and its effect on the Capacity of Multi-Element Antenna Systems," *IEEE Trans. Commun.*, vol. 48, pp. 502–513, 2000.

[10] H. Boelcskei, D. Gesbert, and A. J. Paulraj, On the Capacity of OFDM-Based Multiantenna Syst., 2000, submitted for publication.

[11] W. C. Y. Lee, "Effects on correlation between two mobile radio base-station antennas," *IEEE Trans. Commun.*, vol. 21, pp. 1214–1224, 1973.

[12] J. Fuhl, A. F. Molisch, and E. Bonek, "Unified channel model for mobile radio systems with smart antennas," *Proc. Inst. Elect. Eng.–Radar, Sonar, and Navigation*, vol. 145, pp. 32–41, 1998.

[13] H. Boelcskei and A. J. Paulraj, "Space-frequency coded broadband OFDM systems," in *Proc. IEEE Wireless Communications Network Conf.*, 2000, pp. 1–6.

[14] D. Gesbert, H. Bolcskei, D. Gore, and A. J. Paulraj, "MIMO wireless channels: Capacity and performance prediction," in *Proc. Globecomm 2000*, San Francisco, CA, 2000, pp. 1083–1088.

[15] D. Chizhik, G. J. Foschini, and R. A. Valenzuela, "Capacities of multi-element transmit and receive antennas: Correlations and keyholes," *Electron. Lett.*, vol. 36, pp. 1099–1100, 2000.

[16] W. J. Choi and J. M. Cioffi, "Space-time block codes over frequency selective Rayleigh fading channels," in *Proc. IEEE VTC 1999—Fall*, Amsterdam, 1999, pp. 2541–2545.

[17] U. Martin, J. Fuhl, I. Gaspard, M. Haardt, A. Kuchar, C. Math, A. F. Molisch, and R. Thomä, "Model scenarios for intelligent antennas in cellular mobile communication systems—Scanning the literature," *Wireless Personal Comm., Special Issue on Space Division Multiple Access*, vol. 11, pp. 109–129, 1999.

[18] R. Thomae, D. Hampicke, A. Richter, G. Sommerkorn, A. Schneider, U. Trautwein, and W. Wirnitzer, "Identification of time-variant directional mobile radio channels," *IEEE Trans. Instrum. Meas.*, vol. 49, pp. 357–364, 2000.

[19] M. Steinbauer, D. Hampicke, G. Sommerkorn, A. Schneider, A. F. Molisch, R. Thomae, and E. Bonek, "Array measurement of the double-directional mobile radio channel," presented at the Proc. IEEE Vehicular Technology Conf. Spring 2000—Tokyo, Piscataway, NJ, 2000.

[20] H. Krim and M. Viberg, "Two decades of array signal processing research: The parametric approach," *IEEE Signal Processing Mag. (Special Issue on Array Processing)*, vol. 13, pp. 67–94, July 1996.

[21] E. Bonek and M. Steinbauer, "Double-directional channel measurements," in *Proc. Int. Conf. Antennas Propagation 2001*, Manchester, U.K., 2001, pp. 226–230.

[22] A. G. Richter, D. Hampicke, G. Sommerkorn, and R. Thoma, "Joint estimation of DoD, time-delay, and DoA for high-resolution channel sounding," presented at the Proc. IEEE VTC2000, Spring, 2000.

[23] M. Haardt and J. Nossek, "Unitary ESPRIT: How to obtain increased estimation accuracy with a reduced computational burden," *IEEE Trans. Signal Processing*, vol. 43, pp. 1232–1242, 1995.

[24] R. Roy and T. Kailath, "ESPRIT—Estimation of signal parameters via rotational invariance techniques," *IEEE Trans. Accoustics, Speech, and Signal Processing*, vol. ASSP-37, pp. 984–995, July 1989.

[25] R. A. Horn and C. R. Johnson, *Matrix Analysis*. Cambridge, U.K.: Cambridge Univ. Press, 1985.

[26] M. Steinbauer, A. F. Molisch, and E. Bonek, "The double-directional radio channel," *IEEE Antennas and Propagat. Mag.*, pp. 51–63, Aug. 2001.

[27] W. C. Jakes, *Microwave Mobile Communications*. Piscataway, NJ: IEEE Press, 1993.

[28] A. G. Burr, "Capacity of adaptive space-time coded systems," presented at the Proc. EPMCC 2001—On CD, Vienna, Austria, 2001.

[29] M. Steinbauer, A. F. Molisch, A. Burr, and R. Thomae, "MIMO channel capacity based on measurement results," in *Proc. ECWT 2000*, Paris, France, 2000, pp. 52–55.

[30] N. Amitay, M. J. Gans, H. Xu, and R. A. Valenzuela, "Effects of thermal noise on accuracy of measured blast capacities," *Electron. Lett.*, vol. 37, pp. 591–592, 2001.

[31] A. G. Burr, "Channel capacity evaluation of multi-element antenna systems using a spatial channel model," presented at the Proc. of Millenium Conf. on Antennas & Propagation (AP'2000) on CD, 2000.

Andreas F. Molisch (S'89–M'95–SM'00) received the Dipl. Ing., Dr. Techn., and the habilitation degrees from the Technical University, Vienna, Austria, in 1990, 1994, and 1999, respectively.

From 1991 to 2001, he was with the Institut fuer Nachrichtentechnik und Hochfrequenztechnik (INTHFT) of the TU Vienna, Vienna, Austria, becoming an Associate Professor, in 1999. From 1999 to 2000, he was on leave to the FTW Research Center for Telecommunications, Vienna. Since March 2001, he has been with the Wireless Systems Research Department at AT&T Laboratories—Research in Middletown, NJ. He has done research in the areas of surface acoustic wave filters, radiative transfer in atomic vapors, atomic line filters, and BS antennas. His current research interests are the measurement and modeling of mobile radio channels, MIMO systems, smart antennas, and wideband wireless systems. He has authored, coauthored or edited two books, five book chapters, some 45 journal papers, and numerous conference contributions.

Dr. Molisch is an editor of the IEEE TRANSACTIONS ON WIRELESS COMMUNICATIONS, and coeditor of an upcoming special issue in the IEEE JOURNAL ON SELECTED AREAS IN COMMUNICATIONS on MIMO and Smart Antennas in *J. Wireless Comm. Mob. Comp.* He has participated in the European research initiatives "COST 231," "COST 259," and "COST 273." He has also been Session Organizer, Session Chairman, and Member of the Program Committee of various international conferences. He is a member of OeVE and VDE. He received the GiT prize, in 1991, the Kardinal Innitzer prize, in 1999, and an INGVAR award, in 2001.

Martin Steinbauer (S'99–A'01) was born in Vienna, Austria, in 1973. In 1996, he received the Dipl.-Ing. degree from Technische Universität Wien, Vienna, Australia, with distinction.

After studies on GSM1800 behavior at high vehicular speeds, he joined the Institut für Nachrichtentechnik und Hochfrequenztechnik at TU-Wien, Vienna, Austria, as a Research Engineer. During his three year participation in the EU-project META-MORP, he specialized in radio channel measurement and characterization. As Chairman of a subgroup on directional channel modeling within the European research initiative COST259, he promoted harmonization among different channel modeling approaches toward a common setting for directional channel simulations. His main interests are now on the propagation side of MIMO systems including appropriate measurement techniques, data evaluation and signal processing.

Mr. Steinbauer is a member of the Austrian Electrical Engineering Society.

Martin Toeltsch (S'00) received the Dipl.-Ing. degree (M.S.) in communications engineering (highest honors) from the Technische Universität Wien, Vienna, Austria (TU-Wien), in 1998. He is currently working toward the Ph.D. degree.

From 1992 to 1998, he worked in the field of signal and image processing for medical applications. His research now focuses on OFDM and radio channel measurements, as well as propagation and channel modeling.

Mr. Toeltsch has been a member of the Mobile Communications Group at the Institut für Nachrichten- und Hochfrequenztechnik (INTHF), TU-Wien, since 1998.

Ernst Bonek (M'73–SM'85) was born in Vienna, Austria, in 1942. He received the Dipl.Ing. and Dr.techn. degrees (highest honors) from the Technische Universität Wien (TU Wien), Vienna, Austria.

In 1984, he was appointed Full Professor of Radio Frequency Engineering at the TU Wien. His field of interest is mobile communications at large. Recent contributions concern smart antennas, the characterization of mobile radio channels, and advanced antennas and receiver designs. Altogether, he authored or coauthored some 150 journals and conference publications. He holds several patents on mobile radio technology.

Mr. Bonek has served the IEEE Austria Section as a Chairman, from 1985 to 1990. From 1991 to 1994, he was a Council Member of the Austrian Science Fund, acting as Speaker for engineering sciences. From 1996 to 1999, he served on the Board of Directors of the reorganized Post and Telekom Austria. He participated in the European research initiative COST 259 as Chairman of the working group on Antennas and Propagation, and continues to serve in this position in COST 273. In URSI, he is presently Chairman of Commission C "Signals and Systems". He is an Area Editor of "Wireless Personal Communications".

Reiner S. Thomä (M'93–SM'99) was born in Germany, in 1952. He received the Dipl.-Ing., Dr.-Ing., and the Dr.-Ing. habil. degrees, all in electrical engineering (information technology) from Technische Universität Ilmenau, Ilmena, Germany, in 1975, 1983, and 1989, respectively.

Since 1992, he has been a Professor of Electrical Engineering (Electronic Measurement) and since 1999, he has been the Director of the Institut für Kommunikations- und Meßtechnik at the Technische Universität Ilmenau. His research interests include measurement and digital signal processing methods (correlation and spectral analysis, system identification, array methods, time-frequency, and cyclostationary signal analysis) and their application in mobile radio and radar systems (propagation measurement and directional channel parameter estimation, and ultra-wide-band radar).

Mr. Thomä is a Chairman of the IEEE Instrumentation and Measurement Society Technical Committee TC-13 "Wireless and Telecommunications".